Presumably it was some GaSb–Ga mixture.

Summary

The pyrolysis of TVSb has been investigated in a flow tube reactor using D_2 and He carrier gases. For TVSb alone, the most likely pyrolysis reaction involves an Sb-centered reductive elimination pathway. A less likely possibility is pyrolysis via homolysis of the Sb–C bonds, yielding vinyl radicals. Unfortunately, examination of the organic byproducts in both He and D_2 yields insufficient information to form a definitive hypothesis. However, in He the pyrolysis rate for TVSb is more rapid than for TMSb. Since vinyl radicals form stronger bonds than methyl radicals, this datum contradicts the Sb–C bond homolysis mechanism. Again, the activation energy for pyrolysis is less than the expected Sb–vinyl bond strength. Finally, the addition of C_7D_8 produces no CH_2=CHD, indicative of the absence of vinyl radicals. To elucidate our understanding of GaSb growth by using TMGa and TVSb, the pyrolysis rates for this combination of reactants were also studied. CH_3 radicals from $(CH_3N)_2$ pyrolysis were found to enhance TVSb pyrolysis in He. TMGa also increases the TVSb pyrolysis rate, mainly due to the methyl radicals produced. A heterogeneous pyrolysis reaction appears at high surface area. At V/III ratios normally used for OMVPE growth, carbonaceous deposits were formed. Thus, TVSb may be a useful precursor for OMVPE only at V/III ratios less than unity.

Acknowledgment. We acknowledge financial support from the Office of Naval Research, the Office of Naval Technology, and the Air Force Office of Scientific Research.

Registry No. TVSb, 5613-68-3; TMGa, 1445-79-0.

Structural Chemistry and Raman Spectra of Niobium Oxides

Jih-Mirn Jehng and Israel E. Wachs*

Zettlemoyer Center for Surface Studies, Department of Chemical Engineering, Lehigh University, Bethlehem, Pennsylvania 18015

Received May 29, 1990. Revised Manuscript Received November 5, 1990

A series of niobium oxide reference compounds were investigated by Raman spectroscopy in order to determine the relationship between niobium oxide structures and their corresponding Raman spectra. The assignments of the Raman bands were based on the known niobium oxide structures. The Raman studies indicate that the Raman frequencies strongly depend on the niobium oxide structures. For the slightly distorted octahedral NbO_6 structures ($KNbO_3$, $NaNbO_3$, and $LiNbO_3$), the major Raman frequencies appear in the 500–700-cm^{-1} region. For the highly distorted octahedral NbO_6 structures ($K_8Nb_6O_{19}$, $AlNbO_4$, and $Nb(HC_2O_4)_5$), the major Raman frequencies shift from the 500–700- to the 850–1000-cm^{-1} region. The distortions in the niobium oxide compounds are caused by the corner- or edge-shared NbO_6 octahedra. Both slightly distorted and highly distorted octahedral NbO_6 sites coexist in the $KCa_2Na_{n-3}Nb_nO_{3n+1}$, n = 3–5, layered compounds. Most of the niobium oxide compounds possess an octahedrally coordinated NbO_6 structure with different extents of distortion, and only a few rare-earth $ANbO_4$ (A = Y, Yb, Sm, and La) compounds possess a tetrahedrally coordinated NbO_4 structure. For the tetrahedral NbO_4 structure of $YbNbO_4$ the major Raman frequency appears at ~813 cm^{-1}. In situ Raman studies assisted in the discrimination between bulk and surface functionalities in the niobium oxide reference compounds possessing high surface areas ($Nb_2O_5 \cdot nH_2O$ and $HCa_2Nb_3O_{10}$).

Introduction

Niobium oxide, Nb_2O_5, has been reported to exist in different polymorphic forms,[1-4] and the phase transformations of niobium oxide strongly depend on the heat treatment. Upon heat treatments between 300 and 1000 °C, amorphous niobium oxide increases in degree of crystallinity and forms more stable Nb_2O_5 phases. Amorphous niobium oxide, $Nb_2O_5 \cdot nH_2O$, possesses distorted NbO_6 octahedra, NbO_7 pentahedra, and NbO_8 hexahedra as structural units.[5] The TT-Nb_2O_5 phase, 300–500 °C, possesses a pseudohexagonal unit cell, with a constitutional defect of an oxygen atom per unit cell, and forms tetragonal and pentagonal bipyramids[1] with six or seven oxygen atoms coordinated to the Nb atom. The T-Nb_2O_5 phase, 700–800 °C, possesses an orthorhombic unit cell and forms distorted tetragonal or pentagonal bipyramids with six or seven oxygen atoms coordinated to the Nb atom. One out of seventeen Nb atoms occupies the interstitial sites between two unit cells and is surrounded by eight oxygen atoms.[6] These polyhedra are joined by corner or edge sharing in the *ab* plane and by corner sharing along the *c* axis. The H-Nb_2O_5 phase, above 1000 °C, is the most thermodynamically stable form of the Nb_2O_5 polymorphs. The structure of H-Nb_2O_5 contains two different sizes of ReO_3-type blocks: 3 × 4 and 3 × 5 blocks composed of corner- or edge-shared NbO_6 octahedra. Only 1 out of 28 Nb sites is a tetrahedron.[7]

The niobium oxide structure can be modified by cation substitution into the crystalline lattice to form different kinds of niobium oxide compounds: perovskite structure,[8-10] layered structure,[11-13] and $Nb_6O_{19}^{8-}$ clusters.[14-16]

(1) Ikeya, T.; Senna, M. *J. Non-Cryst. Solids* **1988**, *105*, 243.
(2) Izumi, F.; Kodama, H. *Z. Anorg. Allg. Chem.* **1978**, *440*, 155.
(3) McConnell, A. A.; Anderson, J. S.; Rao, C. N. R. *Spectrochimica Acta* **1976**, *32A*, 1067.
(4) Weissman, J. G.; Ko, E. I.; Wynblatt, P.; Howe, J. M. *Chem. Mater.* **1989**, *1*, 187.
(5) Aleshina, L. A.; Malnenko, V. P.; Phouphanov, A. D.; Jakovleva, N. M. *J. Non-Csyst. Solids* **1986**, *87*, 350.
(6) Kato, K.; Tamura, S. *Acta Crystallogr.* **1975**, *B31*, 673.
(7) Gatehouse, B. M.; Wadsley, A. *Acta Crystallogr.* **1964**, *17*, 1545.

0897-4756/91/2803-0100$02.50/0

These modifications enhance the physical and chemical properties of niobium oxide. The perovskite niobium oxide compounds are used in various fields of materials science such as glasses[17,18] and ceramics,[19,20] and the layered niobium oxide compounds undergo intercalation reactions with organic amines.[21] Nb_2O_5 also reacts with oxalic acid to form niobium oxalate complexes which can exist in aqueous solution.[22] The above niobium oxide compounds possess an octahedrally coordinated NbO_6 structure with different extents of distortion. The tetrahedrally coordinated NbO_4 structure is not a typical structure for niobium oxide because the Nb^{5+} atom is too large to fit into an oxygen-anion tetrahedron. Only a few rare-earth $ANbO_4$ (A = Y, Yb, Sm, and La) compounds have been found to possess tetrahedral coordination.[23-25]

Raman spectroscopy is very sensitive to the structure and bond order of metal oxides, especially in the region of metal–oxygen stretching modes, because many of the Raman frequencies depend on the bond order in the structure.[3] A higher metal–oxygen bond order, corresponding to a shorter bond distance, shifts the Raman bond to higher wavenumbers. In this study, various niobium oxide reference compounds are characterized by Raman spectroscopy and divided into two main categories: the octahedrally coordinated and the tetrahedrally coordinated niobium oxide compounds. The octahedrally coordinated niobium oxide compounds consist of slightly distorted niobium oxides, highly distorted niobium oxide structures, layered structures, and pure niobium oxide. Tetrahedrally coordinated $ANbO_4$ (A = Y, Yb, Sm, and La) compounds have been reported by Blasse,[23] Rooksby et al.,[24] and Yoshida et al.[25] to possess a slightly distorted scheelite structure with NbO_4 units, and only $YNbO_4$ has previously been characterized by Raman spectroscopy. In the present study $YbNbO_4$ was used as the niobium oxide reference compound containing a tetrahedrally coordinated NbO_4 structure. The niobium oxide structure–Raman spectroscopy relationships developed for the reference compounds will subsequently be used to assign the molecular structures of the surface niobium oxide phases in supported niobium oxide catalysts.

Experimental Section

Materials. Hydrated niobium pentoxide, $Nb_2O_5 \cdot nH_2O$, was provided by Niobium Products Co. (Pittsburgh, PA) with a minimum purity of 99.0%. The major impurities after calcining at 800 °C are 0.02% Ta and 0.01% Cl. Niobium oxalate was also provided by Niobium Products Co. with the chemical analysis of 20.5% Nb_2O_5, 790 ppm Fe, 680 ppm Si, and 0.1% insoluble solid.

The $BNbO_3$ (B = Li, Na, and K) compounds were obtained from Johnson Matthey Chemicals Co. with a purity greater than 99.99%. Potassium niobate, $K_8Nb_6O_{19}$, was obtained from Pfaltz and Bauer, Inc. The $KCa_2Na_{n-3}Nb_nO_{3n+1}$ (n = 3–5) compounds were provided by A. Jacobson of Exxon Research and Engineering Co.; the detailed synthesis procedures of these layered oxides were described by Jacobson et al.[13] The hydrated $HCa_2Nb_3O_{10}$ layered oxide was also provided by A. Jacobson. The dehydrated $HCa_2Nb_3O_{10}$ layered oxide was prepared by drying the hydrated $HCa_2Nb_3O_{10}$ layered oxide at 120 °C for 16 h.

BET Surface Area Measurement. The BET surface areas of bulk niobium oxide samples were obtained with a Quantsorb surface area analyzer (Quantachrome Corp. Model OS-9) using a 3:7 ratio of N_2/He mixture as a probe gas. Typically, 0.200–0.300 g of sample was used for the measurement, and the sample was outgassed at 250 °C prior to N_2 adsorption.

Raman Spectroscopy. Raman spectra were obtained with a Spex triplemate spectrometer (Model 1877) coupled to an EG&G intensified photodiode array detector, which were cooled thermoelectrically to −35 °C, and interfaced with an EG&G OMA III optical multichannel analyzer (Model 1463). The samples were excited by the 514.5-nm line of the Ar^+ laser with 10 mW of power. The laser beam was focused on the sample illuminator, where the sample typically spins at about 2000 rpm to avoid local heating, and was reflected into the spectrometer by a 90° angle with the incident light. The scattered Raman light was collected by the spectrometer at room temperature and analyzed with an OMA III software package. The overall spectral resolution of the spectra was determined to be about 2 cm^{-1}. The detailed schematic diagram of the Raman spectrometer is described elsewhere.[26]

An in situ quartz cell was designed in order to investigate the Raman changes upon dehydration of the niobium oxide samples above room temperature. The sample holder was made from a quartz glass, and the sample disk was held by a stationary slot in the sample holder. The sample was heated by a cylindrical heating coil surrounding the quartz cell, and the temperature was measured with an internal thermocouple. The cell was capable of operating up to 600 °C. Reaction gas mixtures were introduced into the cell from a manifold at a rate of 50–500 cm^3/min with a delivery pressure of 150–200 Torr.

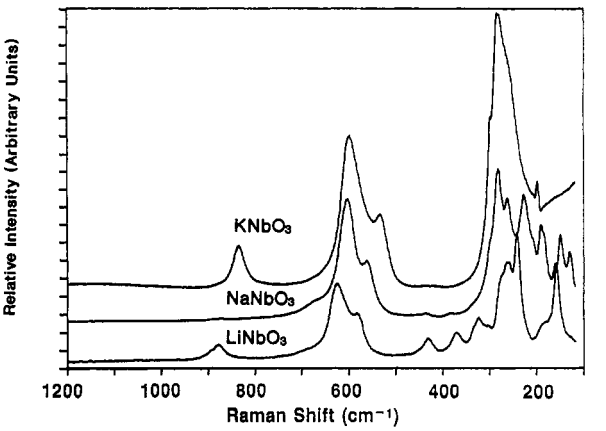

Figure 1. Raman spectra of the $BNbO_3$ (B = Li, Na, K) compounds.

Results

(a) Octahedrally Coordinated Niobium Oxide Compounds. Slightly distorted niobium oxides: The Raman spectra of the $BNbO_3$ (B = Li, Na, and K) reference compounds are shown in Figure 1. The major Raman

(8) Megaw, H. D., *Acta Crystallogr.* **1968**, *A24*, 589.
(9) Sakowski-Cowley, A. C.; Lukaszwicz, K.; Megaw, H. D. *Acta Crystallogr.* **1969**, *B25*, 851.
(10) Katz, L.; Megaw, H. D. *Acta Crystallogr.* **1967**, *22*, 269.
(11) Dion, M.; Ganne, M.; Tournoux, M. *Mater. Res. Bull.* **1981**, *16*, 1429.
(12) Jacobson, A. J.; Johnson, J. W.; Lewandowski, J. T. *Inorg. Chem.* **1985**, *24*, 3727.
(13) Jacobson, A. J.; Lewandowski, J. T.; Johnson, J. W. *J. Less-Common Met.* **1986**, *116*, 137.
(14) Farrell, F. J.; Maroni, V. A.; Spiro, T. G. *Inorg. Chem.* **1969**, *8*, 2638.
(15) Tobias, R. S. *Can. J. Chem.* **1965**, *43*, 1222.
(16) Rocchiccioli-Deltcheff, C.; Thouvenot, R.; Dabbabi, M. *Spectrochim. Acta* **1977**, *33A*, 143.
(17) Glass, A. M.; Nassau, K.; Negran, J. T. *J. Appl. Phys.* **1978**, *49*, 1075.
(18) El Jazouli, A.; Viala, J. C.; Parent, C.; Hagenmuller, P. *J. Solid State Chem.* **1988**, *73*, 433.
(19) Jang, S. J.; Uchino, K.; Nomura, S.; Cross, L. E. *Ferroelectrics* **1980**, *27*, 31.
(20) Swartz, S. L.; Shrout, T. R. *Mater. Res. Bull.* **1982**, *17*, 1245.
(21) Jacobson, A. J.; Johnson, J. W.; Lewandowski, J. T. *Mater. Res. Bull.* **1987**, *22*, 45.
(22) Jehng, J. M.; Wachs, I. E. *ACS Div. Petrol. Chem. Prepr.* **1989**, *34*, 546.
(23) Blasse, G. *J. Solid State Chem.* **1973**, *7*, 169.
(24) Rooksby, H. P.; White, E. A. D. *Acta. Crystallogr.* **1963**, *16*, 888.
(25) Yoshida, S.; Nishimura, Y.; Tanaka, T.; Kanai, H.; Funabiki, T. *Catal. Today* **1990**, *8*, 67.
(26) Wachs, I. E.; Hardcastle, F. D.; Chan, S. S. *Spectroscopy* **1986**, *1*, 30.

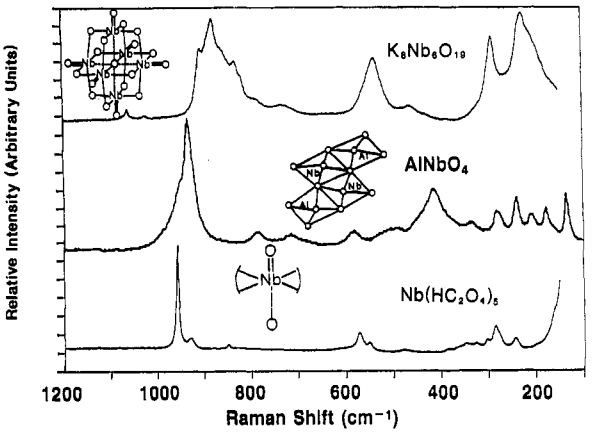

Figure 2. Raman spectra of the highly distorted niobium oxide compounds.

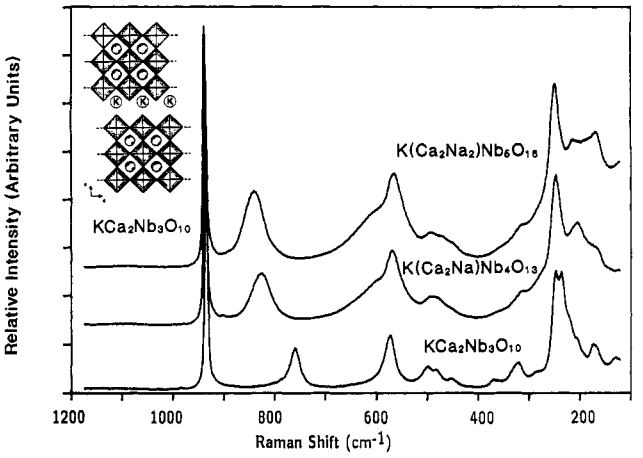

Figure 3. Raman spectra of the $KCa_2Na_{n-3}Nb_nO_{3n+1}$ (n = 3–5) layered oxide compounds.

band of these reference compounds appears in the 620–630-cm^{-1} region, and a shoulder appears in the 520–580-cm^{-1} region. The $LiNbO_3$ compound possesses additional Raman bands at ~870, ~430, ~375, and ~325 cm^{-1}. However, the intensity of these Raman bands is significantly decreased for the $NaNbO_3$ compound and are essentially absent for the $KNbO_3$ compound. For the $KNbO_3$ compound, an additional Raman band is observed at ~840 cm^{-1}. Multiple and strong Raman bands in the low-wavenumber region, between 100 and 300 cm^{-1}, are also observed for these reference compounds.

Highly distorted niobium oxides: The Raman spectra of the $K_8Nb_6O_{19}$, $AlNbO_4$, and $Nb(HC_2O_4)_5$ reference compounds are shown in Figure 2. In the high-wavenumber region (800–1000 cm^{-1}), $K_8Nb_6O_{19}$ possesses Raman bands at ~900, ~880, and ~840 cm^{-1}, $AlNbO_4$ has a Raman band at ~930 cm^{-1}, and $Nb(HC_2O_4)_5$ possesses a Raman band at ~960 cm^{-1}. In the intermediate-wavenumber region (400–800 cm^{-1}), the major Raman band of these niobium oxide compounds appears at ~540 ($K_8Nb_6O_{19}$), ~420 ($AlNbO_4$), and ~570 cm^{-1} ($Nb(HC_2O_4)_5$). Additional Raman bands at ~580, ~730, and ~780 cm^{-1} are observed for $AlNbO_4$. In the low-wavenumber region (100–300 cm^{-1}), $K_8Nb_6O_{19}$ and $Nb(HC_2O_4)_5$ have Raman bands at ~230 and ~290 cm^{-1} and $AlNbO_4$ has Raman bands at ~275, ~240, ~210, and ~180 cm^{-1}.

Layered oxides: The Raman spectra of the $KCa_2Na_{n-3}Nb_nO_{3n+1}$ (n = 3–5) layered oxide reference compounds are presented in Figure 3. The major Raman band of these layered oxides appears at ~930 cm^{-1}. Additional Raman bands at ~760, ~575, and 300–500 cm^{-1} are also present for the $KCa_2Nb_3O_{10}$ compound. A shift of the Raman band from ~760 to ~825 cm^{-1} is observed upon increasing the number of layers from three to four, and this band further shifts to ~840 cm^{-1} as the number of layers is increased to five. The Raman bands at ~450 and ~375 cm^{-1} disappear for the compounds possessing three and four layers.

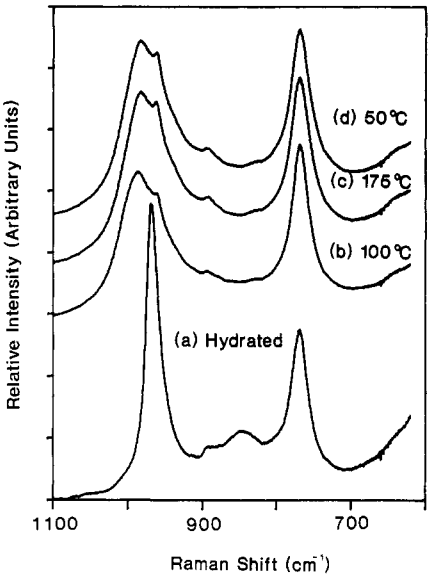

Figure 4. In situ Raman spectra of the $HCa_2Nb_3O_{10}$ layered oxide compound: (a) hydrated state; (b) heated at 100 °C under flowing oxygen; (c) heated at 175 °C under flowing oxygen; (d) cooled to 50 °C under flowing oxygen.

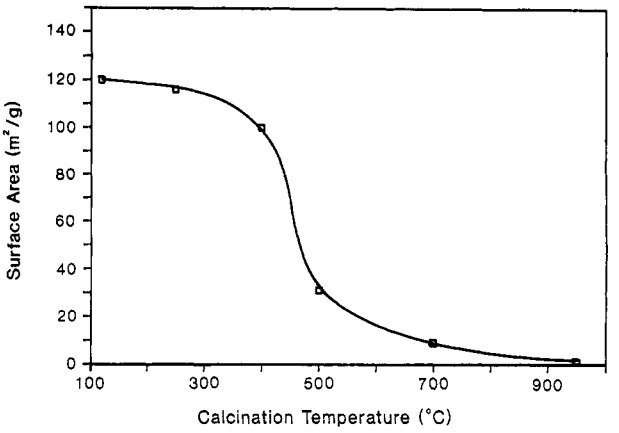

Figure 5. Surface area of bulk niobium oxide as a function of calcination temperature.

The dehydrated state of the $HCa_2Nb_3O_{10}$ layered oxide was investigated by in situ Raman spectroscopy under flowing oxygen, and the results are shown in Figure 4. The ~930-cm^{-1} Raman band for the $KCa_2Nb_3O_{10}$ compound, Figure 3, shifts to ~965 cm^{-1} for the hydrated $HCa_2Nb_3O_{10}$ compound. Upon dehydration, the strong Raman band at ~965 cm^{-1} splits into two bands at ~980 and ~960 cm^{-1}, and the weak Raman band at ~840 cm^{-1} disappears.

Bulk niobium oxide (Nb_2O_5): The surface area of bulk niobium oxide after different thermal treatments in presented in Figure 5. The results show that the niobium oxide surface area dramatically decreases with increasing calcination temperature due to the formation of larger Nb_2O_5 crystallites. The Raman spectra of bulk niobium oxide after thermal treatments from 120 to 1000 °C are shown in Figure 6. For $Nb_2O_5 \cdot nH_2O$ dried at 120 °C for 16 h, a broad and weak Raman band is observed at ~900 cm^{-1} as well as a broad and strong Raman band at ~650

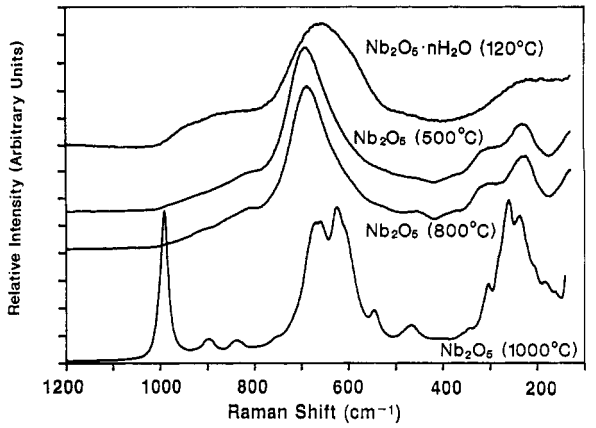

Figure 6. Raman spectra of bulk niobium oxide as a function of calcination temperatures.

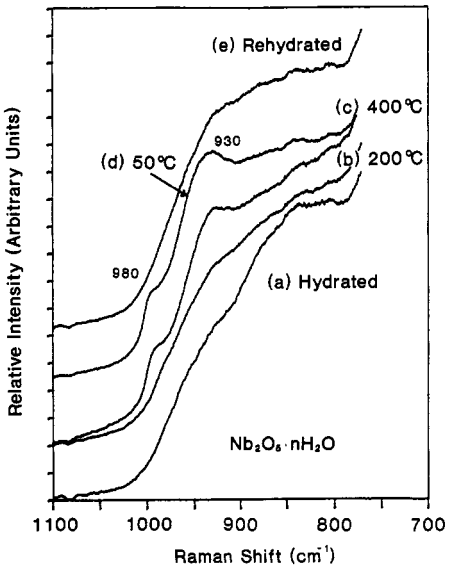

Figure 7. In situ Raman spectra of $Nb_2O_5 \cdot nH_2O$: (a) hydrated state; (b) heated at 200 °C under flowing oxygen; (c) heated at 400 °C under flowing oxygen; (d) cooled to 50 °C under flowing oxygen; (e) readsorbed water molecules under ambient conditions.

cm^{-1}. When the niobium oxide sample is heated for 2 h at 500 °C in air, the broad Raman band at ~900 cm^{-1} becomes even weaker and the strong Raman band at ~650 cm^{-1} shifts to ~690 cm^{-1}. The Nb_2O_5 (500 °C) Raman bands in the low-wavenumber region (200–300 cm^{-1}) become more intense and better resolved than those of $Nb_2O_5 \cdot nH_2O$ (120 °C) in this region. The Raman features of the Nb_2O_5 sample treated at 800 °C for 2 h are similar to those of the Nb_2O_5 (500 °C) sample. However, additional weak Raman bands in the 400–500-cm^{-1} region are observed in the Nb_2O_5 (800 °C) sample. For the Nb_2O_5 sample treated at 1000 °C for 2 h, the Raman results indicate that a phase transformation of the Nb_2O_5 sample has occurred and additional Raman bands are observed in the spectrum (particularly in the high-wavenumber region between 900 and 1000 cm^{-1}). The different Nb_2O_5 phases are also confirmed by X-ray diffraction.[27] $Nb_2O_5 \cdot nH_2O$ (120 °C) is found to be poorly crystalline, showing a diffuse pattern of either monoclinic Nb_2O_5 or $NbO_{2.432}$ (oxygen-deficient Nb_2O_5). Nb_2O_5 (500 °C) and Nb_2O_5 (800 °C) are similar, matching well-crystlline orthorhombic Nb_2O_5. Nb_2O_5 (1000 °C) is very crystalline as well, indicating a mixture of monoclinic phases of Nb_2O_5.

(27) Jehng, J. M.; McCaslin, P. C.; Wachs, I. E., to be published.

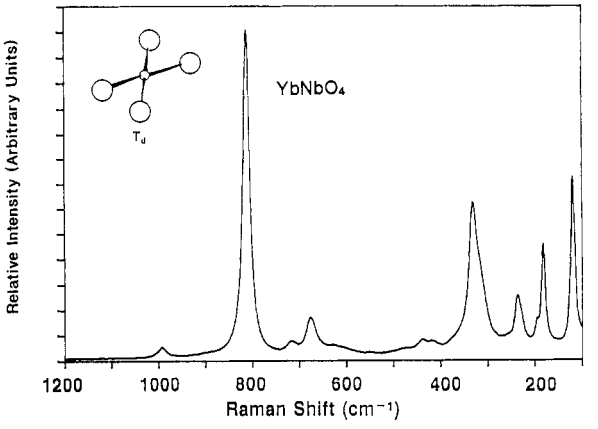

Figure 8. Raman spectrum of the $YbNbO_4$ compound.

Table I. Relationships between Niobium Oxide Structures and Raman Frequencies

struct	Raman bands, cm^{-1}	compounds
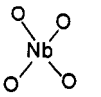	790–830	$YNbO_4$, $YbNbO_4$
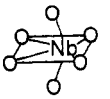	500–700	Nb_2O_5 (amorphous, TT, T, and H), $LiNbO_3$, $NaNbO_3$, $KNbO_3$, layered oxides
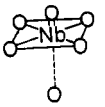	850–1000	$AlNbO_4$, $K_8Nb_6O_{19}$, $Nb(HC_2O_4)_5$, layered oxides

In situ Raman studies of the high surface area $Nb_2O_5 \cdot nH_2O$ (120 °C) sample were also undertaken in order to discriminate between bulk and surface functionalities,[26] and the spectra in the 700–1100-cm^{-1} region are presented in Figure 7. For the untreated $Nb_2O_5 \cdot nH_2O$ (120 °C), a broad Raman band is observed in the 800–900-cm^{-1} region. For the $Nb_2O_5 \cdot nH_2O$ (120 °C) treated at 200 °C for 1 h, the Raman features remain broad and are somewhat similar to the untreated $Nb_2O_5 \cdot nH_2O$ (120 °C). Two new Raman bands, however, are observed at ~930 and ~980 cm^{-1} after thermal treatment at 400 °C for 1 h. These two Raman bands are still present after cooling to 50 °C. However, these two Raman bands disappear after the sample is rehydrated by exposure to ambient water vapor overnight. The major niobium oxide Raman band remained at ~650 cm^{-1} during this thermal treatment and indicates that the $Nb_2O_5 \cdot nH_2O$ sample did not undergo phase transformations.

(b) Tetrahedrally Coordinated Niobium Oxide Compound. The Raman spectrum of $YbNbO_4$ is shown in Figure 8. Raman studies reveal that $YbNbO_4$ possessing Raman bands at ~813, ~331, ~717, and ~435 cm^{-1}. Raman bands at ~992, ~678, ~630, and ~237 cm^{-1} indicate that $YbNbO_4$ also possesses a structure similar to that of H-Nb_2O_5 (see Figure 6). The Raman bands below 200 cm^{-1} are due to lattice vibrations.

Discussion

Most of the niobium oxide compounds contain an octahedral NbO_6 structure with different extents of distortions present in the structures. Niobium oxide compounds containing a tetrahedral NbO_4 structure are extremely rare. The major Raman frequencies of the niobium oxide compounds with the corresponding structures are classified in Table I. A higher niobium–oxygen bond order, corre-

sponding to a shorter bond distance, shifts the Raman band to higher wavenumbers. Every niobium oxide compound in this study has a unique Raman spectrum that is related to the symmetry and bond order of its structure. The Raman band assignments are based on the corresponding Nb–O bond order and known structure.

The tetrahedral NbO_4^{3-} species does not exist in aqueous solutions because of the high electronegativity and small radius of the oxygen atom.[28] In addition, the tetrahedral NbO_4 structure is rarely found in niobium oxide compounds because the Nb^{5+} atom is usually too large to fit into an oxygen-anion tetrahedron.[23] The rare-earth $ANbO_4$ (A = Y, Sm, and La) compounds have been investigated by Blasse[23] and Rooksby et al.,[24] and they determined that these compounds possess NbO_4 tetrahedra that appear to be isomorphous with the scheelite $CaWO_4$ structure. Blasse[23] studied the $YNbO_4$ compound by Raman spectroscopy and predicted the vibrational modes of a regular NbO_4 tetrahedron with no interactions and distortions to occur at 816 (ν_1), 650 (ν_3), 420 (ν_4), and 340 cm^{-1} (ν_2). Yoshida et al.[25] investigated the $YbNbO_4$ compound by XANES and EXAFS techniques and determined that the $YbNbO_4$ compound possesses a NbO_4 tetrahedron. The $ANbO_4$ (A = Y, Yb, Sm, and La) compounds were further studied by Kinzhibalo et al.[29] and Trunov et al.,[30] who determined that these compounds possess a fergusonite structure at room temperature. In the fergusonite structure, the coordination number of the Nb atom contains four oxygen atoms with distances of 1.83–1.93 Å and two further oxygen atoms with distances of 2.40–2.52 Å as a result of the connection between two adjacent tetrahedra. The transition from the octahedral fergusonite to the tetrahedral scheelite depends on temperature. An increase in temperature results in bonds breaking between the niobium atom and the two further oxygen atoms, and the Nb atom coordination becomes tetrahedral.

For the $ANbO_4$ (A = Y, Yb, Sm, and La) compounds, the transition temperature from the octahedral fergusonite to the tetrahedral sheelite depends on the ionic radius of the rare-earth metal. The rare-earth metal possessing a small ionic radius has a high phase transition temperature because of the relatively short bond distances between the niobium atom and the two further oxygen atoms. Thus, the rare-earth $ANbO_4$ (A = Y, Yb, Sm, and La) compounds possess NbO_6 octahedra at room temperature, and transition from a NbO_6 octahedron to a NbO_4 tetrahedron occurs at high temperature. For example, the phase transitions of the $YNbO_4$ and the $YbNbO_4$ compounds occur above 825 °C.[30] Blasse[23] did not address the $YNbO_4$ structures as a function of temperature. The multiple Raman bands appearing in the 400–800-cm^{-1} region for the $YNbO_4$ compound reported by Blasse[23] are probably due to the simultaneous presence of NbO_4 tetrahedra and NbO_6 octahedra in the structure.

Raman studies of the annealed $YbNbO_4$ compound reveal bands at ~813, ~717, ~435, and ~331 cm^{-1}. The Raman bands appearing at ~813 and ~331 cm^{-1} are due to the Nb–O symmetric modes of the NbO_4 tetrahedral structure, and Raman bands appearing at ~717 and ~435 cm^{-1} are due to the Nb–O antisymmetric modes of the NbO_4 tetrahedral structure. This is consistent with Blasse's results that the vibrational modes of a regular NbO_4 tetrahedra, with no interactions and distortions, should occur at 816 (ν_1), 650 (ν_3), 420 (ν_4), and 340 cm^{-1} (ν_2).[23] Additional weak Raman bands appearing at ~992, ~678, ~630, and ~237 cm^{-1} indicate that the $YbNbO_4$ compound also contains an impurity of H-Nb_2O_5 due to a small excess of niobium oxide in the sample. Thus, tetrahedrally coordinated niobium oxide reference compounds possess their major Raman bands in the 790–830-cm^{-1} region.

It appears that the Nb^{5+} is also too small to form a regular octahedral NbO_6 structure,[31] and the oxygens in a regular octahedral NbO_6 structure do not obey Pauling's electrostatic valence rule.[32] Consequently, the niobium oxide compounds predominantly contain NbO_6 octahedra with different extents of distortion due to corner or edge-shared NbO_6 polyhedra.

The $BNbO_3$ (B = Na and K) compounds belong to the perovskite structure family. The Nb atom lies at each corner of a cubic cell, and the oxygen atom lies at the center of each cubic edge. Each Nb atom is surrounded by six oxygen atoms to form a NbO_6 octahedron and two adjacent NbO_6 octahedra are connected by a shared corner. The cation (Na or K) lies in the center of the cubic cell. In an ideal perovskite structure all NbO_6 octahedra would be perfectly regular with the cation (Na or K) surrounded by 12 oxygens and Nb by 6 oxygens. However, such an ideal perovskite structure does not exist in the $BNbO_3$ (B = Na and K) compounds because of the tilting of the NbO_6 octahedra as well as the displacements of the Nb atoms from the center which is induced by the cation (Na or K) and the unbalanced interatomic forces present in the perovskite structures.[8]

The perovskite $BNbO_3$ (B = Na and K) compounds possess a major Raman band at 620–630 cm^{-1} and a shoulder in the 520–580-cm^{-1} region (Figure 1). These bands correspond to slightly different Nb–O bond distances and are assigned to the symmetric stretching mode of the NbO_6 octahedra of these perovskite compounds. The $LiNbO_3$ compound contains a hexagonal close-packed structure in which the regular NbO_6 octahedra are connected by shared corners with a 30° tilting angle between two adjacent NbO_6 octahedra and a 0.26 Å off-center displacement of the Nb atom.[8] The $LiNbO_3$ compound possesses similar Raman features as the perovskite $BNbO_3$ (B = Na and K) compounds in the 500–700-cm^{-1} region. For the $LiNbO_3$ (hexagonal close packing) Raman spectrum, the additional Raman band at ~870 cm^{-1} is assigned to the antisymmetric stretching mode of the Nb–O–Nb linkage, and the associated bending modes of the Nb–O–Nb linkage appear at ~430 and ~375 cm^{-1}. For the $NaNbO_3$ (perovskite) compound, however, the intensity of the Raman bands at ~870, ~430, and ~375 cm^{-1} significantly decrease. This is probably due to the lower tilt angle, 18°, between the adjacent NbO_6 octahedra.[9] Furthermore, the disappearance of these Raman bands in the $KNbO_3$ (perovskite) Raman spectrum suggests that no tilting occurs between the adjacent NbO_6 octahedra in this structure and is consistent with Katz et al.'s results.[10] A new Raman band is observed at ~840 cm^{-1} for $KNbO_3$, which is characteristic of the symmetric stretching mode of the Nb–O–Nb collinear bond present in the structure. The distortions of the $BNbO_3$ (B = Li, Na, and K) compounds depend on the size of the A cations. For the larger size cation such as K the cation is coordinated to 12 oxygens, and free space is unavailable for the NbO_6 octahedra

(28) Muller, M.; Dehand, J. *Bull. Soc. Chim. Fr.* **1971**, *8*, 2837.
(29) Kinzhibalo, L. A.; Trunov, V. K.; Evdokimov, A. A.; Krongauz, V. G. *Kristallografiya* **1982**, *27*, 43.
(30) Trunov, V. K.; Efremov, V. A.; Velikopodny, Yu. A.; Averina, I. M. *Kristallografiya* **1981**, *26*, 67.
(31) Orgel, L. E. *An Introduction to Transition Metal Chemistry*; Wiley: New York, 1960.
(32) Pauling, L. *The Nature of the Chemical Bond*; Oxford University Press: New York, 1952.

to tilt relative to one another. Consequently, the NbO_6 octahedra maintain the parallel orientation. However, the smaller size Li cation only has six coordinated oxygens and forms an octahedral LiO_6 structure. The orientations of the NbO_6 and LiO_6 octahedra induce the tilting between the two adjacent NbO_6 octahedra.[8]

It is known that niobium oxide can exist as $Nb_6O_{19}^{8-}$ clusters in alkaline aqueous solutions and Nb complexes in acidic aqueous solutions as well as precipitates from such solutions. The $Nb_6O_{19}^{8-}$ unit is a well-characterized structure that consists of three different types of Nb–O bonds at each niobium center (see Figure 2): a short Nb=O terminal double bond, a longer Nb–O–Nb bridging bond, and a very long and weak Nb---O bond connected to the center of the cagelike octahedral structure.[14-16] From the known structure of $K_8Nb_6O_{19}$, the main frequencies of the $K_8Nb_6O_{19}$ Raman spectrum in Figure 2 can be assigned: Nb=O terminal stretching mode (~900, ~880, and ~840 cm^{-1}), edge-shared octahedral NbO_6 stretching mode (~730, ~540, and ~460 cm^{-1}), Nb---O stretching mode (~290 cm^{-1}), and Nb–O–Nb bending mode (~230 cm^{-1}). The multiple terminal stretching modes present in the high-wavenumber region are due to unequal Nb=O bond lengths that are present in the $K_8Nb_6O_{19}$ structure.

The niobium oxalate structure consists of a $[NbO(OH)(C_2O_4)_2H_2O]$ or $[NbO(C_2O_4)_3]$ unit and water molecules connected by hydrogen bonds.[33-36] The presence of different niobium oxalate units is dependent on the preparation methods. The $[NbO(OH)(C_2O_4)_2H_2O]$ unit has a pentagonal bipyramidal structure with a short Nb=O terminal double bond and a long Nb–OH_2 bond nearly perpendicular to the pentagonal equatorial plane which consists of two bidentate oxalato ligands and a hydroxyl group. The $[NbO(C_2O_4)_3]$ unit also has a pentagonal bipyramidal structure with a short Nb=O terminal double bond and three bidentate oxalato ligands coordinated to the pentagonal equatorial plane. The sharp and strong Raman band at ~960 cm^{-1} in the niobium oxalate Raman spectrum is assigned to the Nb=O terminal double bond, and the Raman band at ~290 cm^{-1} is assigned to the long and weak Nb–OH_2 bond. The Raman band at ~570 cm^{-1} arises from the bidentate oxalato ligands coordinated to the niobium atom which is characteristic of the breathing mode of the Nb–O_2–C_2 bridging bond.

The structure of $AlNbO_4$ consists of highly distorted octahedral NbO_6 and AlO_6, two NbO_6 units and two AlO_6 units, sharing edges together to form a unit cell and linked to the adjacent unit cell by sharing two corners.[37] The Nb–O bond which links to the adjacent unit cell by sharing two corners possesses the shortest bond length, and the Raman band at ~930 cm^{-1} is characteristic of the symmetric stretching mode of this shortest Nb=O terminal double bond. Raman bands in the 400–800-cm^{-1} wavenumber region are assigned to the symmetric and antisymmetric stretching mode of the Nb–O–Nb linkage, and the associated bending modes appear in the low-wavenumber region (200–300 cm^{-1}). Thus, the $K_8Nb_6O_{19}$, $AlNbO_4$, and $Nb(HC_2O_4)_5$ compounds possess a highly distorted octahedral NbO_6 structure with Raman bands appearing in the high-wavenumber region, 850–1000 cm^{-1}, which are characteristic of the symmetric stretching mode of the Nb=O terminal double bond.

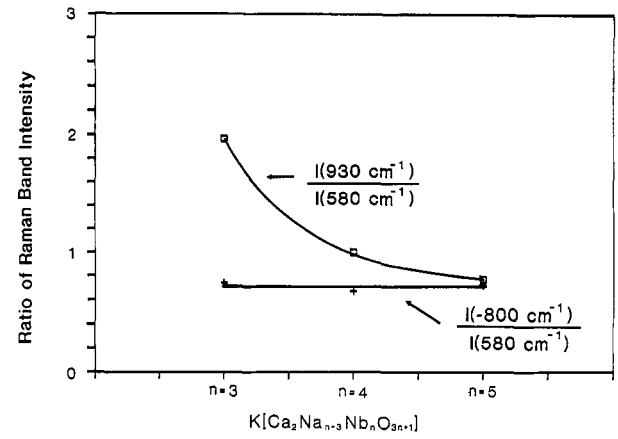

Figure 9. Raman band intensity ratios for the $KCa_2Na_{n-3}Nb_nO_{3n+1}$ (n = 3–5) layered oxide compounds.

The structure of the $K[Ca_2Na_{n-3}Nb_nO_{3n+1}]$ (n = 3–5) layered oxides contains corner-shared NbO_6 octahedra with a large cation occupying 12-coordinated sites in the center of each cube as found in the perovskite structure.[12] The thickness of each perovskite layer is determined by the number of corner-shared NbO_6 octahedra connected along the direction perpendicular to the layers (n = 3–5). The $KCa_2Nb_3O_{10}$ structure has been determined by Dion et al.[11] to possess two types of NbO_6 sites connected to the cations (K and Ca): one is the capping sites between two adjacent layers and the other is the internal sites in the layer.

Raman studies also detect the two types of NbO_6 sites present in the layered oxide compounds: a highly distorted octahedral structure, Raman band at ~930 cm^{-1}, and a slightly distorted octahedral structure, Raman band at ~580 cm^{-1}. The relative concentrations of the two NbO_6 octahedra in the layered oxide compounds can be determined by taking the ratio of these Raman bands (the integrated Raman intensity of the bands at ~930 and ~580 cm^{-1}). The Raman $I(\sim930\ cm^{-1})/I(\sim580\ cm^{-1})$ ratios for the different layered compounds are shown in Figure 9 and decrease with increasing number of niobium oxide layers. For example, the Raman measurements of the layered oxide $KCa_2Nb_3O_{10}$, n = 3, has $I(\sim930\ cm^{-1})/I(\sim580\ cm^{-1})$ = 2, which reflects the ratio of the highly distorted octahedral sites to the slightly distorted octahedral sites. This is consistent with the layered oxide structure described by Dion et al.[11] Upon decreasing the number of the niobium oxide layers, the $I(\sim930\ cm^{-1})/I(\sim580\ cm^{-1})$ ratio further decreases to 1 for $K(Ca_2Na)Nb_4O_{13}$, n = 4, and 0.8 for $K(Ca_2Na_2)Nb_5O_{16}$, n = 5, as expected from the known structures.[12] The quantitative agreement between the Raman ratios and the actual ratios in these layered structures reveals that the Raman cross sections of the slightly distorted and highly distorted NbO_6 octahedra are essentially the same. The Raman $I(\sim800\ cm^{-1})/I(\sim580\ cm^{-1})$ ratios in Figure 9, however, do not change with increasing number of niobium oxide layers. This indicates that the Raman band at ~800 cm^{-1} is associated with the slightly distorted NbO_6 site band at ~580 cm^{-1} and corresponds to different Nb–O bond lengths. Increasing the number of niobium oxide layers also shifts the band from ~760 to ~840 cm^{-1} and eliminates the Raman bands at ~450 and ~375 cm^{-1}. These Raman features reflect the different extents of distortions that exist in the layered oxide compounds and are probably due to the different sizes between the Ca and Na cations.

Many of these layered oxide compounds can also undergo an alkali-metal ion exchange reaction with the protons present in aqueous acidic solutions due to their

(33) Kojic-Prodic, B.; Limingu, R.; Scavnicar, S., *Acta Crystallogr.* **1973**, *B29*, 864.
(34) Galesic, N.; Matkovic, B.; Herceg, M.; Sljukic, M. *J. Less-Common Met.* **1971**, *25*, 234.
(35) Brnicevic, N.; Djordjevic, C. *J. Less-Common Met.* **1971**, *23*, 107.
(36) Mathern Par, G.; Weiss, R. *Acta Crystallogr.* **1971**, *B27*, 1610.
(37) Pedersen, B. F. *Acta Chem. Scand.* **1962**, *16*, 421.

high ionic conductivity. The potassium cation in the layered oxide $KCa_2Nb_3O_{10}$ exchanges with the hydrogen proton in an aqueous acidic solution to form the layered oxide $HCa_2Nb_3O_{10}$. The layered oxide $HCa_2Nb_3O_{10}$ possesses a tetragonal unit cell with an interlayer separation 14.38 Å, which is contracted relative to the values of 14.73 Å observed for the layered oxide $KCa_2Nb_3O_{10}$.[13] When hydrogen replaces potassium, the interlayer hydrogen stabilizes the terminal oxygen atoms by forming a terminal -OH group interacting with a terminal oxygen in the adjacent layer. The stoichiometry corresponds to one proton for every pair of terminal oxygens from the adjacent layers. The hydrated $HCa_2Nb_3O_{10}$ compound has a composition $HCa_2Nb_3O_{10}\cdot 1.5H_2O$ with an interlayer separation 16.23 Å. The interlayer hydrogen bonding between the two adjacent terminal oxygens creates some free volume in the $HCa_2Nb_3O_{10}$ structure to accommodate 1.5 water molecules.[13]

The in situ Raman studies of the layered oxide $HCa_2Nb_3O_{10}$ indicate that the Nb=O terminal double bond is affected by the adsorbed water since the Raman band at ~965 cm^{-1} broadens and splits into two bands at ~980 and ~960 cm^{-1} upon dehydration (see Figure 4). The Raman band at ~840 cm^{-1} is assigned to the Nb=O antisymmetric stretching mode, which is better resolved in the hydrated state. Thus, the in situ Raman studies demonstrate that the water molecules in the layered oxide $HCa_2Nb_3O_{10}$ structure associate with all the interlayered terminal oxygens to form Nb=O---H bonds. The results are in agreement with the structural studies of Jacobson et al.[13] The in situ Raman studies of the layered oxide $HCa_2Nb_3O_{10}$ also reveal that hydrogen bonding via water molecule addition results in a decrease in the Nb=O bond order and its corresponding vibrational frequency.

Bulk Nb_2O_5 undergoes the following phase transformations during heat treatments:[38-40]

$$\text{amorphous } Nb_2O_5\cdot nH_2O \xrightarrow[300\text{-}500\ ^\circ C]{} \text{TT-}Nb_2O_5 \xrightarrow[700\text{-}800\ ^\circ C]{} \text{T-}Nb_2O_5 \xrightarrow[>1000\ ^\circ C]{} \text{H-}Nb_2O_5$$

The amorphous $Nb_2O_5\cdot nH_2O$ contains slightly distorted NbO_6, NbO_7, and NbO_8 polyhedra.[1] The strong and broad Raman band at ~650 cm^{-1} is assigned to the symmetric stretching mode of the niobia polyhedra. The broad Raman feature reflects the distribution of the NbO_6, NbO_7, and NbO_8 sites in the structure of the amorphous $Nb_2O_5\cdot nH_2O$. The weak and broad Raman band at ~900 cm^{-1} is assigned to the symmetric stretching mode of the Nb=O surface sites because of the response of this band to surface dehydration during the in situ Raman studies (see following paragraph). Heat treatment at 500 °C for 2 h leads to crystallization into the TT-Nb_2O_5 phase. The corresponding shift of the Raman band from ~650 to ~690 cm^{-1} is due to the increasing bond order of the niobia polyhedra, and the sharpening of Raman band at ~690 cm^{-1} is due to the more ordered structure present in the TT-Nb_2O_5 phase. The TT-Nb_2O_5 phase contains octahedral and pentagonal bipyramid structures, and the weak Raman band at ~900 cm^{-1} is due to the small concentration of Nb=O surface sites after the thermal treatment. Additional Raman bands in the low-wavenumber region, 200–300 cm^{-1}, are also observed in the TT-Nb_2O_5 spectrum, which are characteristic of the bending modes of the Nb–O–Nb linkages. Raman features of the T-Nb_2O_5 (800 °C) phase are similar to those of the TT-Nb_2O_5 (500 °C) phase (see Figure 6). This indicates that the T-Nb_2O_5 (800 °C) phase possesses a structure similar to that of the TT-Nb_2O_5 (500 °C) phase and is consistent with Weissman et al.'s conclusions that the TT-Nb_2O_5 and T-Nb_2O_5 phases possess nearly identical structures.[4]

The H-Nb_2O_5 phase contains 3 × 4 and 3 × 5 blocks of corner- or edge-shared octahedral NbO_6 as well as 1 tetrahedral site per 28 Nb sites. Bhide et al.[41] have assigned the Raman band in the high-wavenumber region, 900–1200 cm^{-1}, to the Nb=O terminal bond. Therefore, Raman bands at ~997 and ~900 cm^{-1} for the H-Nb_2O_5 phase in Figure 6 are characteristic of the symmetric and antisymmetric stretching modes of the Nb=O terminal bond. Blasse[23] studied the $YNbO_4$ compound by Raman spectroscopy and determined that the tetrahedral NbO_4 possesses a major Raman band at 830 cm^{-1}. McConnell et al.[3] and Iwasawa et al.[42] referred to Blasse's result and determined that the Raman band at 840 cm^{-1} in H-Nb_2O_5 is due to the tetrahedral NbO_4 structure. This assignment is not correct because Blasse did not address that the transition of $YNbO_4$ from the octahedral fergusonite to the tetrahedral scheelite depends on temperature.[30] In addition, the Nb–O bond distances of the tetrahedral site in H-Nb_2O_5 have been determined to be 1.65 and 1.68 Å by Gatehouse et al.[7] The predicted Raman frequency with corresponding Nb–O bond distance of the H-Nb_2O_5 tetrahedral site appears at 993 cm^{-1} by using Hardcastle's bond distance/frequency correlation with the overall uncertainty of 30 cm^{-1}.[43] Thus, the Raman band at 840 cm^{-1} for H-Nb_2O_5 can not be assigned to the NbO_4 tetrahedron. The corner-shared octahedral NbO_6 in the H-Nb_2O_5 phase forms a Nb–O–Nb collinear bond with a corresponding Raman band appearing at ~840 cm^{-1}.[1] Raman bands in the 500–800-cm^{-1} region are characteristic of the stretching modes of the slightly distorted octahedral NbO_6 structures. At the low-temperature treatments (<800 °C), the structure of niobium oxide possesses the slightly distorted octahedral niobia polyhedra. The structure of the niobium oxide treated at high temperatures, greater than 1000 °C, possesses a highly distorted octahedral NbO_6 structure in addition to the slightly distorted octahedral NbO_6 structure. Thus, the phase transformations of niobium oxide are strongly dependent on the heat treatments, and this is reflected in the Raman spectra.

During in situ Raman experiment the samples are heated to desorb the adsorbed moisture, and those Raman features that respond to the dehydration treatment are identified as surface functionalities.[44] This process is reversed by readsorbing water vapor on the surface functionalities. The in situ Raman studies of $Nb_2O_5\cdot nH_2O$ (see Figure 7) demonstrate that the broad and weak Raman bands in the 800–900-cm^{-1} region shift to higher frequencies due to thermal desorption of the adsorbed moisture. After dehydration of $Nb_2O_5\cdot nH_2O$ at 400 °C in air for 1 h, two new Raman bands are observed at ~930 and ~980 cm^{-1} which are characteristic of two different Nb=O surface sites. No phase transformations occurred during this thermal treatment since the Raman features of bulk niobium oxide remained the same. The concentration of the Nb=O terminal sites of bulk Nb_2O_5 (pretreated at 500 °C) is too small to be observed due to the much lower surface area. Thus, the amorphous $Nb_2O_5\cdot nH_2O$ material

(38) Brauer, G. *Z. Anorg. Allg. Chem.* **1941**, 248, 1.
(39) Schafer, H.; Breil, G. *Z. Anorg. Allg. Chem.* **1952**, *267*, 265.
(40) Schafer, H.; Gruehn, R.; Schulte, F. *Angew. Chem.* **1966**, *78*, 28.
(41) Bhide, V.; Husson, E. *Mater. Res. Bull.* **1980**, *15*, 1339.
(42) Nishimura, M.; Asakura, K.; Iwasawa, Y. *J. Chem. Soc., Chem. Commun.* **1986**, 1660.
(43) Hardcastle, F. D. Dissertation, Lehigh University; University Microfilms International: Ann Arbor, MI, 1990.
(44) Chan, S. S.; Wachs, I. E.; Murrell, L. L.; Wang, L.; Hall, W. K. *J. Phys. Chem.* **1984**, *88*, 5831.

possesses terminal Nb=O sites on the surface, and the number of terminal Nb=O sites can be eliminated by high-temperature calcinations which dramatically decreased the surface area. The in situ Raman studies confirm the presence of the terminal Nb=O surface sites on amorphous $Nb_2O_5 \cdot nH_2O$ and the assignment of the Raman band at ~900 cm^{-1} to the terminal Nb=O surface sites.

Conclusions

The relationships between niobium oxide structures and their corresponding Raman spectra were systematically studied for various types of niobium oxide compounds. The Raman frequencies strongly depend on the bond order of the niobium oxide structure. A higher niobium–oxygen bond order, corresponding to a shorter bond distance, shifts the Raman frequency to higher wavenumbers. Most of the niobium oxide compounds possess an octahedrally coordinated NbO_6 structure, slightly or highly distorted. Only a few niobium oxide compounds (such as $YNbO_4$, $YbNbO_4$, $LaNbO_4$, and $SmNbO_4$) can possess a tetrahedrally coordinated NbO_4 structure that is similar to the scheelite-like structure. For the tetrahedral NbO_4 structure, the major Raman frequency appears in the 790–830-cm^{-1} region. For the slightly distorted octahedral NbO_6 structure, the major Raman frequencies appear in the 500–700-cm^{-1} wavenumber region. For the highly distorted octahedral NbO_6 structure, the Raman frequency shifts from the 500–700- to the 850–1000-cm^{-1} region. Both slightly distorted and highly distorted octahedral NbO_6 sites coexist in the $KCa_2Na_{n-3}Nb_nO_{3n+1}$, n = 3–5, layered compounds. The distortions in the niobium oxide compounds are caused by the formation of corner- or edge-shared NbO_6 octahedra.

Acknowledgment. Financial support for this work by Niobium Products Company Inc. is gratefully acknowledged. We wish to thank A. Jacobson of Exxon Research and Engineering Co. for providing the layered niobium oxide compounds and S. Yoshida of Kyoto University, Japan, for providing the $YbNbO_4$ compound.

Registry No. $KNbO_3$, 12030-85-2; $NaNbO_3$, 12034-09-2; $LiNbO_3$, 12031-63-9; $K_8Nb_6O_{19}$, 12031-11-7; $AlNbO_4$, 12258-25-2; $Nb(CH_2O_4)_5$, 12404-95-4; $K(Ca_2Na_2)Nb_5O_{16}$, 98820-43-0; $K(Ca_2Na)Nb_4O_{13}$, 98820-40-7; $KCA_2Nb_3O_{10}$, 80487-87-2; $HCa_2Nb_3O_{10}$, 98820-36-1; Nb_2O_5, 1313-96-8; $Nb_2O_5 \cdot nH_2O$, 12326-08-8; $YbNbO_4$, 12034-62-7.

Phase-Transfer Palladium(0)-Catalyzed Polymerization Reactions. 6. Synthesis and Thermotropic Behavior of Mono- and Difluorinated 1,2-Bis(4-*n*-alkoxyphenyl)acetylene Monomers†

Coleen Pugh and Virgil Percec*

Department of Macromolecular Science, Case Western Reserve University, Cleveland, Ohio 44106

Received May 30, 1990

Symmetrically difluorinated 1,2-bis(3-fluoro-4-*n*-alkoxyphenyl)acetylene (n = 4–12) and asymmetric, monofluorinated 1-(3-fluoro-4-*n*-alkoxyphenyl)-2-(4-*n*-alkoxyphenyl)acetylene (n = 5–12) monomers were prepared by a one-pot, phase-transfer Pd(0)/Cu(I)-catalyzed three-step coupling of the appropriate aryl halides with 2-methyl-3-butyn-2-ol. All odd members of the 1,2-bis(3-fluoro-4-*n*-alkoxyphenyl)acetylene series are crystalline with a virtual nematic mesophase. All even members of the series present monotropic nematic mesophases. The thermotropic behavior of the 1-(3-fluoro-4-*n*-alkoxyphenyl)-2-(4-*n*-alkoxyphenyl)acetylenes changes continuously with n. The n = 5 derivative is crystalline. The n = 6–10 derivatives each have an enantiotropic nematic mesophase. In addition, the n = 7, 8 derivatives exhibit an enantiotropic smectic mesophase, and the n = 9, 10 derivatives exhibit monotropic smectic C mesophases. Both the nematic and smectic C mesophases of the n = 11, 12 derivatives are monotropic.

Introduction

In a recent publication,[1] we described a one pot, solid–liquid phase-transfer Pd(0)/Cu(I)-catalyzed synthesis of 1,2-bis(4-alkoxyaryl)acetylenes from aryl halides deactivated by alkoxy substituents. The three-step, one-pot synthesis outlined in Scheme I was adapted from Carpita[2] et al.'s liquid–liquid phase-transfer catalyzed synthesis of diheteroarylacetylenes. In the first step, an aromatic halide is coupled with a monoprotected acetylene. The resulting carbinol derivative is deprotected in the second step with formation of an aryl acetylene, which is then coupled with a second aryl halide in the final step. In this phase-transfer catalyzed (PTC), one-pot procedure, only the final diarylacetylene product is isolated.

The subsequent papers in this series described the thermotropic behavior of both symmetrically and asymmetrically substituted 1,2-bis(4-alkoxyaryl)acetylene monomers.[3-5] The linear 1,2-bis(4-*n*-alkoxyphenyl)acetylenes

† Part 5: Pugh, C.; Tarnstrom, C.; Percec, V. *Mol. Cryst. Liq. Cryst.*, in press.

* To whom correspondence should be sent.

(1) Pugh, C.; Percec, V. *J. Polym. Sci., Polym. Chem. Ed.* **1990**, *28*, 1101.
(2) Carpita, A.; Lessi, A.; Rossi, R. *Synthesis* **1984**, 571.
(3) Pugh, C.; Percec, V. *Mol. Cryst. Liq. Cryst.* **1990**, *178*, 193.
(4) Pugh, C.; Percec, V. *Polym. Bull.* **1990**, *23*, 177.
(5) Pugh, C.; Tarnstrom, C.; Percec, V. *Mol. Cryst. Liq. Cryst.*, in press.

0897-4756/91/2803-0107$02.50/0